Paper Presented at the IIT 2012 Conference – Spain June 16, 2012

# Mass and Charge Overlaps in Beamline Implantation and SIMS Analysis of Compound Semiconductor Materials

M.I. Current[1], R. Eddy[2], C Hudak[2], J. Serfass[3] and G. Mount[3]

*[1]Current Scientific, 1729 Comstock Way, San Jose, CA USA 95124, [2]Core Systems, 1050 Kifer Rd., Sunnyvale, CA 94086 USA, [3]Evans Analytical Group, 810 Kifer Rd., Sunnyvale, CA 95051 USA*

# Mass and Charge Overlaps in Beamline Implantation and SIMS Analysis of Compound Semiconductor Materials

M.I. Current[1], R. Eddy[2], C Hudak[2], J. Serfass[3] and G. Mount[3]

*[1]Current Scientific, 1729 Comstock Way, San Jose, CA USA 95124, [2]Core Systems, 1050 Kifer Rd., Sunnyvale, CA 94086 USA, [3]Evans Analytical Group, 810 Kifer Rd., Sunnyvale, CA 95051 USA*

**Abstract.** Mass overlaps occurring as a result of extraction of ions from an arc discharge and gas collisions producing molecular break up and charge exchange in the accelerator beamline are examined for ion implantation into compound semiconductors. The effect of the choice of plasma gas elements for Be+ implants is examined as an example.

**Keywords:** Compound semiconductors, mass overlaps, charge exchange, $Be^+$ implants.
**PACS:** 61.72, 61.72u, 34.50.-s, 25.60.Lg

## Introduction: Diverse Implants into Diverse Materials

The next steps in the continuing drive to increase IC device performance are set to include a shift to high-mobility channel materials for both planar and finFET devices, these being among the "last knobs" available in the continued quest for increased CMOS transistor and IC device performance [1,2]. The leading high-mobility materials are Ge and various forms of compound semiconductors. This shift will significantly widen the range of elements and ion types in routine use for ion implantation processing.
This paper examines the various forms of elemental, energy and dose "contaminations" that occur with the use of dopants and other ions useful for fabrication of III-V and other compound semiconductor devices, building on similar studies of contaminant ions in implants used for Si-device fabrication [3, 4]. The practical aspects of this study will discuss the effects of the use of various dopant source materials, ion source components and the relative utility of various forms of "mass filters" in beamline accelerator designs.

As in Si-based devices, an increasing number of implants are for non-dopant, "materials modification" implants to facilitate a diverse range of processes, ranging from silicide layer stabilization to multi-exposure resist stabilization [5]. An example of the diversity of the ions being explored for processing of advanced IC materials is shown in Fig. 1, a sample of the recent R&D implants done at Core Systems.

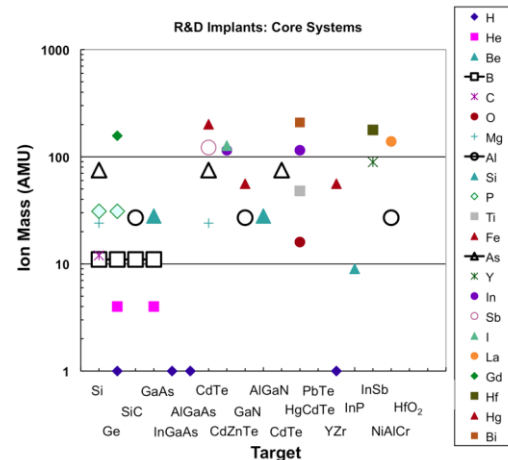


**FIGURE 1.** A sample of recent ions and electronic materials targets implanted at Core Systems.

## Mechanisms for Unintentional Elemental Co-implantation

The principal mechanisms active when unintentional co-implantation occurs are (1) failure of the magnet optics and "mass apertures" to resolve ions with closely matched optical paths in the analyzing magnet [6], (2) passage of multiple ion types and charge states through magnetic mass separation systems following various charge exchange and molecular breakup events [7], (3) vapor transport of contaminant elements to the target surface followed by recoil implantation by the ion beam [8], energy contamination through acceleration of molecular breakup component ions by potential drops after analyzing magnet [9] and (4) acceleration of ions

created by sputtering or arcing in the beamline components in line with the target surface [3, 10]. These mechanisms are sketched in Fig. 2.

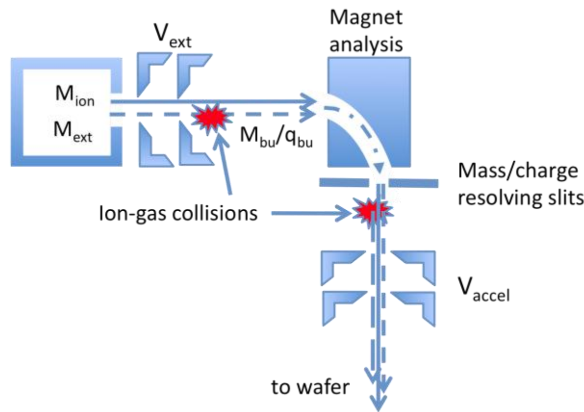


**FIGURE 2**. Sketch of ions in beamline showing the desired ion, $M_{ion}$, extracted from the source plasma, contaminant ions, $M_{ext}$, from the source plasma and $M_{bu}$ after molecular breakup and charge exchange collisions near the extraction and before the final accelerations stages.

Perhaps the most famous of direct overlaps is the contamination of $BF_2^+$ (AMU = 48, 49) beams by $Mo^{+2}$ ions (AMU/q = 46, 47, 47.5, 48, 48.5, 49, 50) sputtered from Mo arc chamber liners and extraction slits in the sources area when the beam is analyzed by a magnet-aperture "mass" filter.

Magnet-aperture beam filters are also vulnerable to a wide range of ion overlaps resulting from charge exchange and molecular breakup events associated with collisions of source ions with background gas atoms in the region between the source extraction and the magnet filter. These overlaps occur when an ion, $m_p^{+a}$, with mass, m, atom count, p and charge a, collides with a background gas atom and continues on as an ion, $m_q^{+b}$, of atom count, g and charge, b. When the beam is filtered with a deflection magnet followed by a small aperture slit, the resulting $m_q^{+b}$ ion has an apparent AMU of $(a/b^2)*(q^2/p)*m$ and an energy of $(q/p)*(aeV)$, where V is the source extraction voltage and e is the electron charge [4]. When the apparent AMU of the $m_q^{+b}$ ion overlaps with the desired ion in the source extraction flow, they are both passed through with same radius of curvature path in the magnet filter and process together to the target. For the general case of a molecular species extracted with a total mass of $m_{ext}$ and charge state, $q_{ext}$, the apparent mass passing through the magnet analysis of the ion resulting from breakup into a mass, $m_{bu}$, with charge state, $q_{bu}$, is $M_{apparent} = (q_{ext}/(q_{bu})^2)*((m_{bu})^2/m_{ext})$.

These effects are particularly prevalent in multi-charged beams that also contain multimer ions in the source extraction current. These linked pairs of multi-charge and multimer ions, commonly called "Aston bands" after the 1922 Nobel prize work done on mass spectroscopy by F.W. Aston but actually first described and explained by H.D. Smyth in 1924 [11], are shown in Fig. 3.

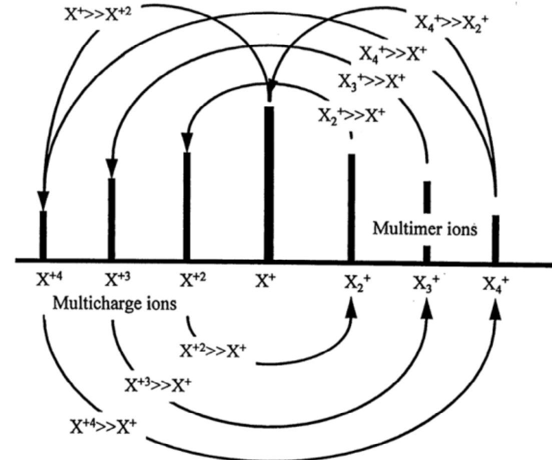


**FIGURE 3.** Ion overlaps for multi-charged and multimer ions after collision-induced charge exchange and multimer breakup events.

An example of charge exchange effects is the beamline transport of $W^{+2}$ ions in $BF_2$+ beams with magnetic selection, where the $W^{+2}$ ions are created by charge striping of $W^+$ ions during collisions after extraction from the source plasma and before the magnet selection [12]. The sources of the $W^+$ ions are sputtering from the arc source filament, extraction slit and chamber wall liners. The transport of the resulting $W^{+2}$ ions near the effective mass of 49 results in no significant W transport when implanting ion beams other than $BF_2^+$. Effects of molecular breakup in contamination of multi-charge ion beams are reviewed in ref. 4, 13 and 14.

## Ions and Carrier Gases with Overlaps

Many of the ions used in the implantation of compound semiconductors are generated with the use of reactive "carrier gases" that do not contain the desired ions. An example is the generation of $Al^+$ ions, for use in implantation of SiC for instance, by reactions of a $BF_3$ carrier gas with an Al oxide or nitride "tablet" placed on the reflector plate of a Bernas/IHC arc source [15]. This method produces a higher and more stable extraction current than the use of Al containing source gases from a vaporizer. However there is a risk in the use of $BF_3$ in the case where there is an air leak, or another source of O

atoms, in the source area with the mass overlap of $Al^+$ (AMU= 27) and $BO^+$ (AMU = 26 and 27) in the extraction current. The good practice used in this case is to use an Al nitride source tablet and B nitride insulators rather than $Al_2O_3$. Note that the use of BN source insulators is not without contamination risk, such as the B ions (AMU = 10, 11) present in a $P^{+3}$ beam (AMU/q = 10.3).

Mass overlaps, resulting either from direct extraction from the arc plasma or from dissociative collisions at the extraction electrode, which are passed by a magnet analysis system with the same apparent mass/charge as common ions used for compound semiconductor processing are shown in Table 1 for 3 common plasma feed gases.

**TABLE 1.** Mass overlaps for ions of interest for implants into compound semiconductors; collisions before magnet

| Extracted ion (AMU) | Dissociated ion (AMU) | Apparent AMU at magnet | Overlap Risk (AMU) |
|---|---|---|---|
| **$SiF_4$ feed gas** | - | - | - |
| $SiF_3^+$ (85) | no collision | 85 | $Rb^+$ (85-87) |
| $SiF_2^+$ (66) | no collision | 66 | $Zn^+$ (64-70) |
| $SiF_4^+$ (104) | $SiF_3^+$ (85) | 47 | $Ga^+$ (69-71) |
| $SiF_4^+$ (104) | $SiF_2^+$ (66) | 41.9 | x |
| $SiF_4^+$ (104) | $SiF^+$ (47) | 21.2 | x |
| $SiF_3^+$ (85) | $SiF_2^+$ (66) | 51.2 | $Cr^+$ ((50-54), $Rh^{+2}$ (103) |
| $SiF_3^+$ (85) | $SiF^+$ (47) | 26 | x |
| $SiF_3^+$ (85) | $Si^+$ (28) | 9.2 | $Be^+$ (9) |
| $SiF_2^+$ (66) | $SiF^+$ (47) | 33.5 | $Ga^{+2}$ (69-71) |
| $SiF_2^+$ (66) | $Si^+$ (28) | 11.9 | $Mg^{+2}$ (24-26) |
| $SiF^+$ (47) | $F^+$ (19) | 7.7 | $Be^+$ (9) |
| $F_4^+$ (76) | $F_3^+$ (57) | 42.7 | $Rb^{+2}$ (96-104) |
| $F_3^+$ (57) | $F_2^+$ (38) | 25.3 | $V^{+2}$ (50-51) |
| $F_2^+$ (38) | $F^+$ (19) | 9.5 | $Be^+$ (9) |
| $F^{+2}$ (19) | no collision | 9.5 | $Be^+$ (9) |
| **$PF_5$ feed gas** | - | - | - |
| $PF_5^+$ (126) | $PF_4^+$ (107) | 90.8 | $Zr^+$ (90-96) |
| $PF_4^+$ (107) | no collision | 107 | $Ag^+$ ((107-109) |
| $PF_4^+$ (107) | $PF_3^+$ (88) | 72.3 | $Nd^{+2}$ (142-150) |
| $PF_4^+$ (107) | $PF_2^+$ (69) | 44.5 | $Y^{+2}$ (89) |
| $PF_4^+$ (107) | $PF_4^+$ (107) | 23.4 | $Ti^{+2}$ (46-50) |
| $PF_4^+$ (107) | $P^+$ (31) | 8.9 | $Be^+$ (9) |
| $PF_4^+$ (107) | $F^+$ (19) | 3.4 | $Li^{+2}$ (6-7) |
| $PF_3^+$ (88) | $PF_2^+$ (69) | 54.1 | $Ag^{+2}$ (107-109) |
| $PF_3^+$ (88) | $PF^+$ (50) | 28.4 | $Fe^{+2}$ (54-58) |
| $PF_2^+$ (69) | no collision | 69 | $La^{+2}$ (138-139) |
| $PF^+$ (50) | $F^+$ (19) | 7.2 | $Li^+$ (6-7) |
| $F_4^+$ (76) | no collision | 76 | $Sm^{+2}$ (144-154) |
| $F^{+2}$ (19) | no collision | 9.5 | $Be^+$ (9) |
| **$BF_3$ feed gas** | - | - | **-** |
| $BF_3^+$ (68) | no collision | 68 | $La^{+2}$ (138-139) |
| $BF_2^+$ (49) | no collision | 49 | $Ti^{+2}$ (46-50) |
| $BF_2^+$ (49) | F+ (19) | 7.4 | $Li^+$ (6-7) |
| $F^{+2}$ (19) | no collision | 9.5 | $Be^+$ (9) |
| $BO^+$ (27) (with O in arc) | no collision | 27 | $Al^+$ (27) |

To illustrate the impact of a mass overlap listed in Table 1, 100 keV, 1.4e14 Be/cm$^2$ $Be^+$ implants were done into GaAs wafers using $SiF_4$ and $PF_4$ as plasma generating gases with a solid foil of Be placed in an arc discharge ion source in a vintage Veeco medium current implanter. The extraction voltage was 35 kV and the acceleration column was at 65 kV. The SIMS profiles from these wafers are shown in Fig. 4.

For the case using $SiF_4$ plasma gas, strong profiles of Si (arising from collisions with background gases at the source extraction electrodes by $SiF_3^+$ ions resulting in $Si^+$ ions with an apparent mass at the magnet of 9.2) and F (arising from $F_2^+$ ions colliding with gas atoms at the extraction stage resulting in $F^+$ ion with an apparent mass of 9.5). There is also a substantial low energy F peak whose origins are at present unknown. The energy, approximately 14 keV, is consistent with neutral F from collisions with the F+ beam at the region of the mass resolving slits. However, the implant tool used here had a vertical beam deflection after the high voltage stage that does not allow for

neutral atom transport to the wafer. The energies for the mass overlap ions are 76.5 keV for $Si^+$ and 82.5 and 14 keV for the $F^+$ ions. Fitting the SIMS peaks with SRIM calculated profiles in GaAs yields doses of 4e13 $Si/cm^2$ for the $Si^+$ ions and 3e12 $F^+/cm^2$ and 6e12 $F^0/cm^2$ for the F contaminants. These strong mass overlap profiles reflect the effects of relatively inefficient vacuum pumping in the extraction and mass analysis regions of the older machine design.

When $PF_5$ is used as the plasma forming gas (see the lower part of Fig.4), no substantial contaminant profiles were seen in the Be implant. The P levels were also below the SIMS detection limits, except for a slight surface peak at about 3e17 $P/cm^3$, perhaps due to recoil implantation of absorbed $PF_5$ vapors.

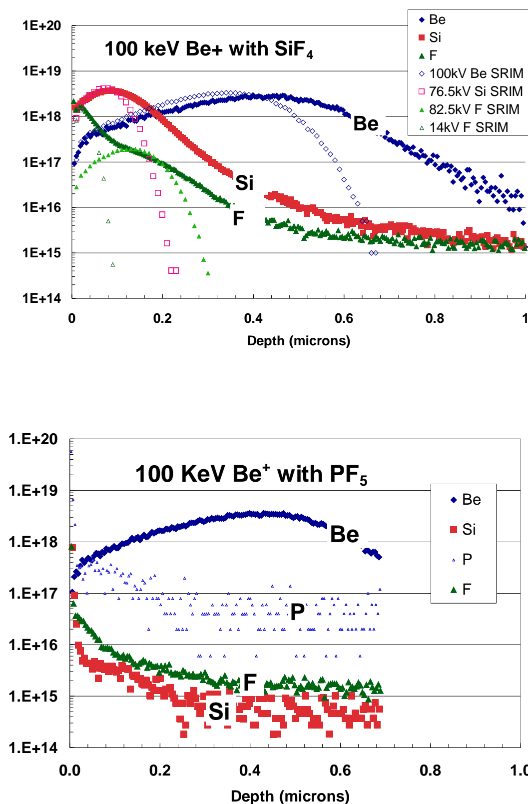


**FIGURE 4.** SIMS profiles of GaAs implanted with 100 keV $Be^+$ at a dose of 1e14 $Be/cm^2$ using carrier gases, $SiF_4$ (upper) and $PF_5$ (lower).

A common countermeasure to prevent co-implantation by mass overlap ions is to operate a "beam filter" to augment the "mass" selection of the magnet and beam aperture stage. However care must be taken to install the filter stage at a point after an accel of decel stage so the lower energy overlap ions can be blocked successfully [16].

## SUMMARY

The increasing use of SiC and GaN for "smart power" switches, added to the broad range of applications for GaAs and related III-V materials in photonic, RF and high-mobility CMOS devices, has led to significant expansion of the ion types used in routine ion implantation. Many of these ion types and ion source operational procedures are prone to risk of atomic and energetic contamination for implantation into compound semiconductors. Careful study of implanted profiles and modeling of potential mass overlaps [17] are required to assure success.

## ACKNOWLEDGMENTS


We acknowledge valuable discussions with M. Naito of Nissin Ion on measures to provide pure ion beams for implants into compound semiconductor devices.


## REFERENCES


1. D.K. Sadana, "CMOS-22 nm and beyond", in "*Ion Implantation Applications, Science and Technology*", ed. J.F. Ziegler, IIT10 schoolbook. (2010).
2. M. Radosavljevic et al., "Electrostatics improvement in 3-D tri-gate over ultra-thin body planar InGaAs quantum well field effect transistors with high-k gate dielectric and scaled gate-to drain/gate-to source separation", IEDM2011.
3. F.A. Stevie et al., "Review of secondary ion mass spectrometry characterization of contamination associated with ion implantation", J. Vac. Sci. Technol. B 12(4) Jul/Aug (1994) 2263-79.
4. M.I. Current, "Ion implantation in silicon device manufacturing: A vacuum perspective", J. Vac. Sci. Technol. A 14(3) May/Jun (1996) 1115-1123.
5. K. Tsukamoto et al., "Evolution of ion implantation technology and its contribution to semiconductor industry", IIT10 (2010), AIP CP1321, 9-16.
6. A.Cubina, M.Frost, "Effects of Molybdenum Contamination Resulting From $BF_2$ Implantation", IIT90. Nuclear Instr and Meth. B55 (1991) 160-165.
7. R.G. Cooks, "Collision-induced dissociation: Readings and commentary", J. Mass. Spectrom. 30 (1995) 1215-1221.
8. J.J.Cummings, D.Enloe, "A RGA Study of the Cross-contamination of Dopant Species and Low Level Impurities and the Use of the RGA as a Process Monitor on the Varian 180XP". IIT90. Nucl. Instr Meth. B55 (1991) 55-60.
9. D.F. Downey, R.B. Liebert, "Control of $BF_2$ dissociation in high-current implantation", IIT90, Nuc. Inst. Meth. B55 (1991) 49-54.

10. J. England, M. McLaren, R. Mitchell, “Elemental analysis of ion implanted added particles”, IIT96, IEEE 96TH8182, (1996), 158-161.
11. H. Budzikiewicz, R.D. Grisby, “Half protons of double charged protons? The history of metastable ions”, J. Am. Soc. Mass Spectrom. 15 (2004) 1261-1265).
12. R.B. Liebert, G.C Angel, M. Kase, “Tungsten contamination in $BF_2$ implants”, IIT96, IEEE Proc. 96TH8182 (1997) 135-138.
13. T. Kubo et al., “Energy contamination from multiple-charged ion implantation in conventional implanter”, IIT96, IEEE Proc.96TH8182 (1997) 100-103.
14. M. Scott-Castle et al., “Characterizing energy contamination mechanisms in multiply charged ion beams”, IIT96, IEEE Proc. 96TH8182 (1997) 111-114.
15. H. Igo et al., “Development of medium current ion implanter ”IMPHEAT” for SiC”, IIT10, AIP Proc. 1321 (2010) 388-391.
16. B. Adibi et al., “Development and application of a beam energy filter for the PI9200XJ high current implanter”, IIT92, Elsevier (1993) 601-606.
17. V. Haublein, H. Ryssel, L. Frey, “Purity of ions beams: Analysis and simulation of mass spectra and mass interferences in ion implantation”, in Advances in Materials Science and Engineering Volume 2012 (2012), Article ID 610150, 9 pages, doi:10.1155/2012/610150.. Also discussed by the same authors in Proc. IIT02, IEEE 02EX505 (2003) 217-220.